Available online at www.sciencedirect.com
ScienceDirect
Journal of Computational Physics 227 (2008) 2105–2117
JOURNAL OF COMPUTATIONAL PHYSICS
www.elsevier.com/locate/jcp

On a new defect of shock-capturing methods

S. Kudriakov [a,*], W.H. Hui [b]

[a] CEA Saclay, DEN/DANS/DM2S/SFME/LTMF, Bat454, 91191 Gif-sur-Yvette Cedex, France
[b] Department of Mechanical Engineering, Hong Kong Polytechnic University, Hong Kong

Received 23 May 2007; received in revised form 17 October 2007; accepted 18 October 2007
Available online 30 October 2007

Abstract

This paper proposes an explanation and a cure (or avoidance) to the new defect found of Eulerian shock-capturing methods in "A note on the conservative schemes for the Euler equations" by Tang and Liu [H. Tang, Tiegang Liu, A note on the conservative schemes for the Euler equations, J. Comput. Phys. 218 (2006) 451–459]. The latter gives a numerical investigation using several popular high resolution conservative schemes applied to Riemann problems of inviscid, compressible, perfect gas flows in Eulerian and Lagrangian coordinates with an initial high density ratio as well as a high pressure ratio. The results show that these methods work very inefficiently when applied to such problems and may give inaccurate numerical results, especially in shock location (or speed), even with a very fine grid.

We have found that in problems of this type a strong rarefaction wave (SRW) is present adjacent to a contact line. Godunov averaging over the wave then produces large errors which, when the wave is strong, also persist for a long time. The cumulative error is thus very large which violates the strength of the contact line adjacent to it which, in turn, affects the speed and hence the location of the shock on the other side of the contact. We confirm this numerically using a method based on the unified coordinates with the shock-adaptive Godunov scheme plus contact strength preserving. The method, when applied to the Examples 2.1 and 2.2 of Tang and Liu [H. Tang, Tiegang Liu, A note on the conservative schemes for the Euler equations, J. Comput. Phys. 218 (2006) 451–459], produces high quality results even for comparatively coarse grids.

MSC: 76A02; 76N10; 76N15; 65M99; 65C20

Keywords: Shock-capturing methods; Unified coordinates; Lagrangian coordinates; Strong rarefaction waves; Contact strength

1. Introduction

Recently, Tang and Liu [1] have reported a new defect with shock-capturing methods applied to Riemann problems using Eulerian *or Lagrangian* formulation when the initial density ratio across a contact line is high: the computed shock location is incorrect no matter how refined the grid is, and the defect appears to be asso-

* Corresponding author. Tel.: +33 1 6908 5285; fax: +33 1 6908 8229.
E-mail address: skudriakov@cea.fr (S. Kudriakov).

0021-9991/$ - see front matter © 2007 Elsevier Inc. All rights reserved.
doi:10.1016/j.jcp.2007.10.014

ciated with the presence of a strong rarefaction wave (SRW). No explanation or cure was offered and the problem remains open.

It is well known that Eulerian shock-capturing methods already have a number of defects, namely, contact smearing, start-up errors, slow-moving shocks, low pressure flows, sonic point glitch, and the notorious wall overheating. A list of such difficulties has been compiled in [2,3]. All these are shown in [4,5] to be either cured or avoided by using the unified coordinates approach, i.e, a generalized Lagrangian coordinates with shock-adaptive Godunov scheme, instead of the conventional Godunov scheme. An explanation to the new defect found in [1] will be given in this paper. Furthermore, it will be shown that this defect can also be cured within the same framework as developed in [4,5], modified so as to preserve the strength of the contact discontinuity adjacent to the rarefaction wave, i.e. to provide the exact values for *all flow variables* at both sides of the contact line.

This paper is organized as follows: In Section 2 we analyze the source of errors causing shock dislocation in the presence of a strong rarefaction wave. Section 3 describes the unified coordinates approach and the contact-strength preserving technique designed to avoid the error source. Numerical examples are presented in Section 4 and compared with those of [1]. Finally, conclusions are given in Section 5.

2. Error source for shock dislocation in the presence of SRW

From what was presented in [1], it is clear that the cause of the defect in shock location lies in the presence of a SRW due to a strong and sudden expansion arising from high initial density ratio. Cell-averaging across the rarefaction wave (RW) thus produces large errors which, when used in the Godunov scheme, gives errors in the strength (and, in Eulerian computation, also location) of the contact which, in turn, cause the shock to move at a wrong speed and hence wrong location. The phenomenon is similar in nature to that occurs in the well-known wall overheating phenomena, which was cured by the method developed in [4,5].

Let us demonstrate this point using the solution to the Riemann problem in Lagrangian coordinates, denoting λ and ξ for the Lagrangian time and the Lagrangian coordinate, respectively, and $\mathbf{Q}$ for the conserved variables. The solution to the Riemann problem

$$\frac{\partial \mathbf{Q}}{\partial \lambda} + \frac{\partial \mathbf{F}}{\partial \xi} = 0 \tag{1}$$

$$\mathbf{Q} = \begin{cases} \mathbf{Q}_L & \text{for } \xi < 0 \\ \mathbf{Q}_R & \text{for } \xi > 0 \end{cases} \tag{2}$$

consists of a shock, a contact and a rarefaction wave. With the use of Lagrangian coordinates, the location of a contact discontinuity can be captured sharply as it always coincides with a coordinate line. However, there is no guarantee that its strength can also be computed correctly if the rarefaction wave is strong.

In the Godunov scheme, the update of flow variables from one time level to the next consists of two steps: (Step 1) solving Riemann problems for every pair of adjacent cells and (Step 2) cell-averaging of the conserved

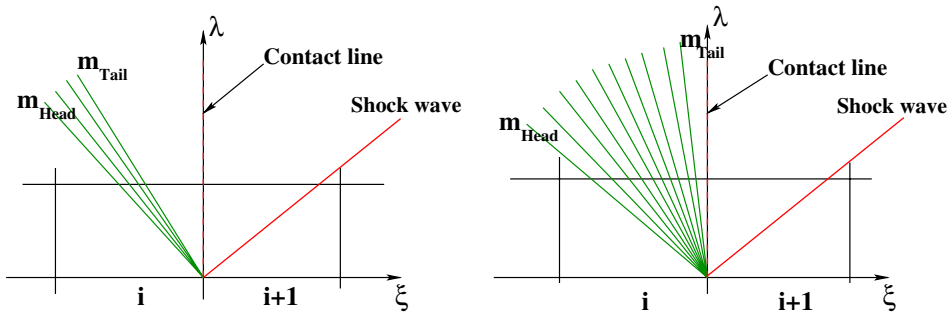

Fig. 1. Solution to a Riemann Problem in Lagrangian coordinates with $\left|\frac{m_{\text{Head}}}{m_{\text{Tail}}}\right| < R$ (left), and $\left|\frac{m_{\text{Head}}}{m_{\text{Tail}}}\right| > R$ (right).

variables. Since the Riemann problems are solved exactly, there is no error at Step 1. However, an error, and the only error, is generated in Step 2 due to cell-averaging of the conserved variables.

Let us consider a left rarefaction wave with the slopes m_{Head} of the head and m_{Tail} of the tail of it (see Fig. 1). A measure of the strength of a RW is

$$r = \left| \frac{m_{\text{Head}}}{m_{\text{Tail}}} \right| \tag{3}$$

When $r < R$ the RW is weak or moderate (Fig. 1, left), and when $r > R$ it is strong (Fig. 1, right). The value of R can be taken equal to 10.0 for the examples given in [1]. With a moderate RW, the averaging error over cell i is small, as the tail of the RW moves with a speed of the same order as the speed of its head. By contrast, with a strong RW, the averaging error over cell i is large and, moreover, this error persists a large number of time steps before the RW leaves the cell, as the speed of the tail of the RW is at least one order of magnitude smaller than the speed of its head. At each time step, the averaging error in cell i gives rise to errors of flow variables in cell $(i+1)$ through the cell interfacial flux. Therefore, in the case of a SRW the cumulative error is large which, in turn, affects the shock speed and hence location.

We shall give more quantitative demonstrations using the three problems from [1].

Problem 1 (*Example* 2.1 *of* [1]). This is a Riemann problem subject to the following initial data for density ρ, velocity u and pressure p.

$$(\rho, u, p) = \begin{cases} (1000, 0, 1000) & \text{if } 0 \leqslant x < 0.3, \\ (1, 0, 1) & \text{if } 0.3 < x \leqslant 1. \end{cases} \tag{4}$$

With high initial density and pressure ratios given, a very strong rarefaction wave is generated in the high pressure region (left) once the diaphragm is removed. For this Riemann problem, the slopes of the head and tail of the RW in Lagrangian coordinates are (the formula for the slope m will be given in the Section 3.1, see (18), and Appendix.)

$$\mathbf{m}_{\text{Head}} = -1.183, \tag{5}$$

$$\mathbf{m}_{\text{Tail}} = -0.0255813, \tag{6}$$

hence $r = 46.245$.

If we multiply $\mathbf{m}_{\text{Tail}}$ by the final time $t = 0.15$ as used in [1], then the distance travelled by the tail of the RW over that time is $d = 0.0038372$. It means that *for a cell size bigger than d the expansion wave did not leave the cell i at the final time t* = 0.15. The Godunov averaging over this cell at every time step will always produce an error in the conservative variables, leading to solving the Riemann problems between the cells i and $(i+1)$ at every time step with incorrect initial data. The cumulative error up to $t = 0.15$ will lead to incorrect flow values on the other side of the contact which, in turn, result in a wrong speed of the shock.

Problem 2 (*Example* 2.2 *of* [1]). This is a Riemann problem subject to the even stringent initial conditions:

$$(\rho, u, p) = \begin{cases} (10000, 0, 10000) & \text{if } 0 \leqslant x < 0.3, \\ (1, 0, 1) & \text{if } 0.3 < x \leqslant 1. \end{cases} \tag{7}$$

Similar to Problem 1, we get

$$\mathbf{m}_{\text{Head}} = -1.183, \tag{8}$$

$$\mathbf{m}_{\text{Tail}} = -0.00588, \tag{9}$$

hence, $r = 201.20$.

Again, if we multiply m_{Tail} by the final time $t = 0.15$ as used in [1], then the distance travelled by the RW tail is $d = 0.000706$, and we encounter the same error in shock speed as in Problem 1.

Problem 3 (*Example* 2.3 *of* [1]). This is a Riemann problem subject to the initial conditions with modest density ratio:

$$(\rho, u, p) = \begin{cases} (445, 0, 1000) & \text{if } 0 \leqslant x < 0.6, \\ (500, 0, 1) & \text{if } 0.6 < x \leqslant 1. \end{cases} \tag{10}$$

In this problem we have

$$\mathbf{m}_{\text{Head}} = -3.1461, \tag{11}$$

$$\mathbf{m}_{\text{Tail}} = -1.501, \tag{12}$$

Hence $r = 2.096$.

If we multiply $\mathbf{m}_{\text{Tail}}$ by the final time $t = 0.3$ as used in [1], then the distance travelled by the RW tail is $d = 0.450$. The RW will leave the cell i long before the final time $t = 0.3$, thus minimizing the cumulative error due to averaging over the wave and leading to an approximately correct contact and correct shock speed (location), as shown in [1].

We note that all the examples from [9] fall in the same category, i.e. the Riemann problems with modest initial density ratio, and ordinary shock-capturing methods can give reasonable results. We also note that for problems of this type the unified coordinates approach in [4,5] gives much improved results.

The above discussions can also explain why the solution to Problem 1 (Example 2.1 of [1]) with the exact initial data taken at $t_0 > 0.001$ can lead to a sufficiently accurate shock location for the particular grid size ($dx = 1/800$). At time $t_0 = 0.002$, the distance between the contact and the tail wave of the RW is $d = 0.000625 = dx/2$. This means that to have *at least one computational cell in the segment between the contact line and the tail of the expansion wave*, one needs $t_0 > 0.002$. This explains why in Fig. 12 of [1] the shock is captured correctly for $t_0 = 0.005$, but not so for $t_0 = 0.001$.

From the above examples we see that the use of *Lagrangian coordinates alone* appears to be insufficient for the resolution of the problem of shock dislocation in the presence of SRW (see also [1], Fig. 9). The key to resolving the difficulty associated with SRW lies in how to avoid the large averaging error from affecting the contact (hence affecting the shock speed and location).

3. The unified coordinates approach

3.1. Classical Lagrangian coordinates versus unified coordinates

The Euler equations of gas dynamics in Eulerian coordinates (t, x) for a perfect gas with a gamma law in 1D flow are

$$\frac{\partial}{\partial t}\begin{pmatrix} \rho \\ \rho u \\ \rho e \end{pmatrix} + \frac{\partial}{\partial x}\begin{pmatrix} \rho u \\ \rho u^2 + p \\ u(\rho e + p) \end{pmatrix} = 0 \tag{13}$$

In (13), γ is the ratio of specific heats of the gas, and

$$e = \frac{u^2}{2} + \frac{p}{(\gamma - 1)\rho} \tag{14}$$

Consider the following transformation [2] to the unified coordinates (λ and ξ)

$$\begin{cases} \mathrm{d}t = \mathrm{d}\lambda \\ \mathrm{d}x = hu\,\mathrm{d}\lambda + A\,\mathrm{d}\xi \end{cases} \tag{15}$$

It can easily be shown that

$$\frac{\partial \xi}{\partial t} + hu\frac{\partial \xi}{\partial x} = 0. \tag{16}$$

This means that the coordinate ξ is invariant following a pseudo-particle whose velocity is hu. It unifies the Eulerian coordinates when $h = 0$ and the Lagrangian when $h = 1$. The classical Lagrangian coordinate system is a special case of the unified coordinate system when we take $A = 1/\rho$ in adition to $h = 1$.

Under transformation (15) with $h = 1$, the system (13) becomes

$$\frac{\partial}{\partial\lambda}\begin{pmatrix}\rho A\\ \rho Au\\ \rho Ae\\ A\end{pmatrix}+\frac{\partial}{\partial\xi}\begin{pmatrix}0\\ p\\ up\\ -u\end{pmatrix}=0 \tag{17}$$

The last equation is the compatibility condition provided by transformation (15). Using the unified coordinates the formula for a slope m of a ray of a rarefaction wave is

$$m=\pm\frac{a}{A},\quad \text{where } a=\sqrt{\frac{\gamma p}{\rho}}. \tag{18}$$

The above equation is used for the calculation of the slopes m_{Head} and m_{Tail} given in the previous section. In the classical Lagrangian formulation, Eq. (17) simplifies to (see also [6]):

$$\begin{cases}\frac{\partial u}{\partial\lambda}+\frac{\partial p}{\partial\xi}=0\\ \frac{\partial e}{\partial\lambda}+\frac{\partial pu}{\partial\xi}=0\\ \frac{\partial}{\partial\lambda}\left(\frac{1}{\rho}\right)-\frac{\partial u}{\partial\xi}=0\end{cases} \tag{19}$$

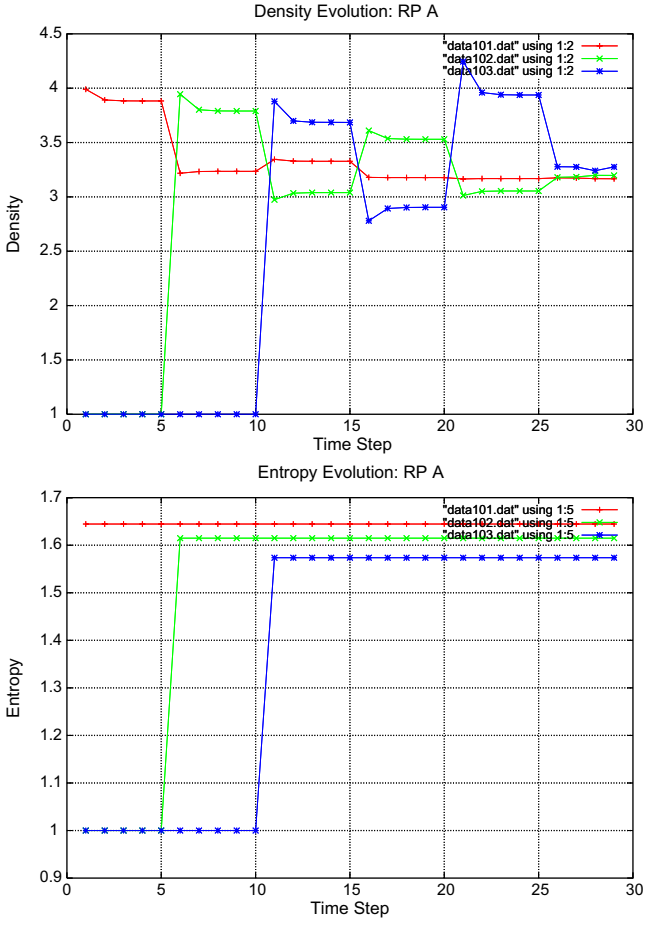

Fig. 2. Problem 1. Density (top) and Entropy (bottom) evolution with time in the cells $(i+1)$ (red), $(i+2)$ (green), and $(i+3)$ (blue). $d\xi = 1/100$. (For interpretation of the references to colour in this figure legend, the reader is referred to the web version of this article.)

A comparision between (17) and (19) shows that formulation using unified coordinates (17) has more flexibility, as A can be chosen freely. In all our computations in this paper, we take $A = \frac{\partial x}{\partial \xi} = 1$ at $\lambda = 0$ to have a *uniform initial grid in the physical space*. An example showing the differences between the classical Lagrangian computation and the unified computation will be given later.

3.2. Shock-adaptive Godunov scheme

With the use of Lagrangian coordinates, the location of contact discontinuity can be captured sharply. In the case of a moderate RW, we can then also resolve the shock sharply by applying the shock-adaptive Godunov scheme introduced in [4,7,8]. We shall take advantage of the fact that the Riemann solution provides us with the exact location of the shock wave. The basic idea of the shock-adaptive Godunov scheme consists of splitting a shock-cell, i.e., a computational cell containing a shock wave, along the trajectory of the shock. The splitted shock-cell becomes two sub-cells: one entirely upstream of the shock and the other entirely downstream. In this way, the cell-averaging procedure across the shock discontinuity, and the error associated with it, are avoided, resulting in infinite shock resolution. The fictitious cell boundary separating the two sub-cells and moving through the regular grid at the local shock speed shall be called a partition. With this partition, the two sub-cells and the other ordinary cells are treated on an equal footing in the Godunov scheme.

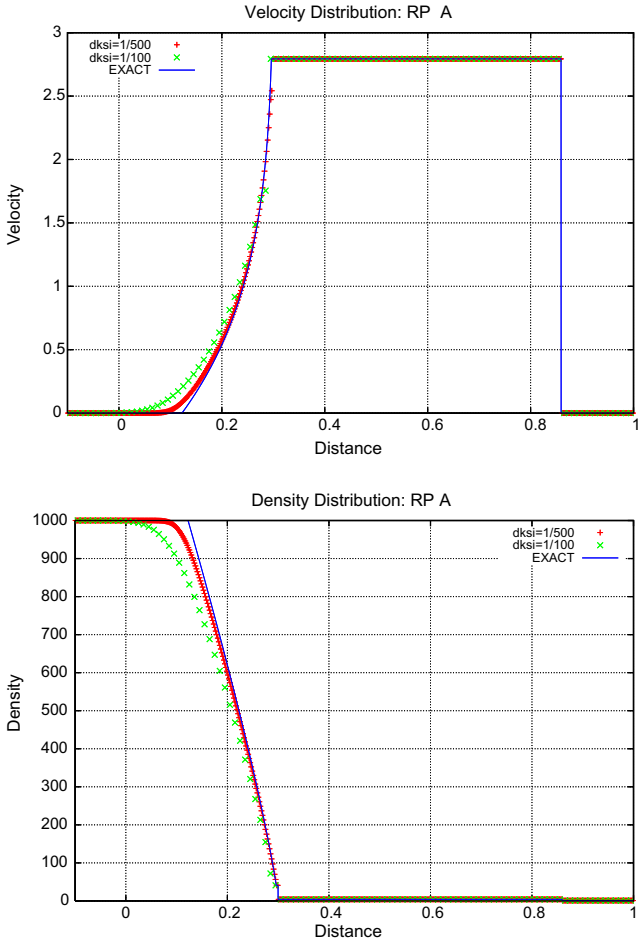

Fig. 3. Problem 1. Solution to a Riemann Problem using the present method. Velocity (top) and density (bottom) distributions are presented in Lagrangian space.

For more details of the shock-adaptive Godunov scheme and its numerical implementation in 1D flow, see [4] and for those in 2D steady flow, see [7,8].

We remark that the shock-adaptive scheme is, in effect, doing a shock-fitting in an overall Godunov shock-capturing method. This costs us no extra effort, since the information needed for fitting a shock is already available in the exact Riemann solution.

Fitting a shock, however, has the important consequence that the Euler equations, (17), need no longer be written in the conservation form, allowing us to use equations in other form.

In this alternative form, the energy conservation equation (the third equation in (17)) is replaced by the entropy conservation equation

$$\frac{\partial S}{\partial \lambda} = 0, \quad \text{where } S = \frac{p}{\rho^{\gamma}} \tag{20}$$

which is valid, as will be used, in the smooth flow region. We note in passing that the Euler equations of gas dynamics for 1D unsteady flow admit four and only four conservation laws—conservation of mass, momentum, energy, and entropy—but only three of them are independent. With the use of Eq. (20) the Euler equations in the unified coordinates become

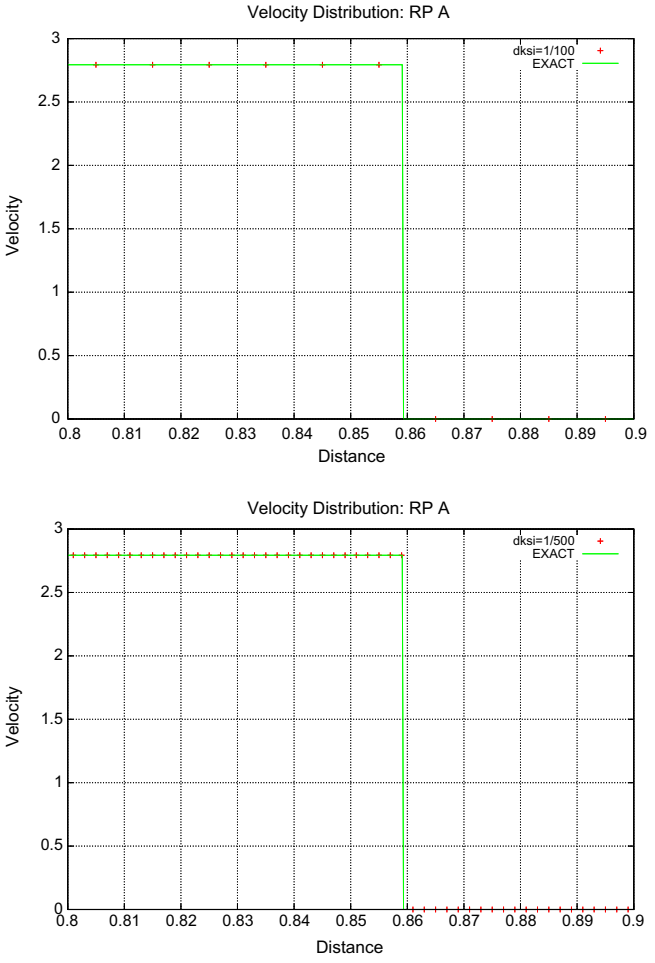

Fig. 4. Problem 1. Close-up of the velocities calculated by the present method with $d\xi = 1/100$ (top) and $d\xi = 1/500$ (bottom).

$$\frac{\partial}{\partial\lambda}\begin{pmatrix}\rho A\\ \rho A u\\ S\\ A\end{pmatrix}+\frac{\partial}{\partial\xi}\begin{pmatrix}0\\ p\\ 0\\ -u\end{pmatrix}=0 \tag{21}$$

which are to be used in the smooth flow region.

The above form of equations enables us to cure the notorious contact overheating problem (see [5]) which can be summarized as follows:

Sudden compression of a gas flow due to shock reflection from a solid wall or sudden expansion due to an abrupt withdrawal of a piston from the gas is often associated with a phenomenon known generically as wall overheating. Most conventional shock-capturing numerical methods accurately predict pressure and velocity, while under-predicting density and thus over-predicting temperature near the wall, hence the name. Due to the entropy conservation Eq. (20) in the smooth flow region we have exact entropy everywhere in the flow field, provided that its initial values at each cell are computed exactly. Finally, this exact entropy, together with the correctly predicted pressure (by most of the shock-capturing methods), correctly predicts the density and hence the temperature, including that at the contact.

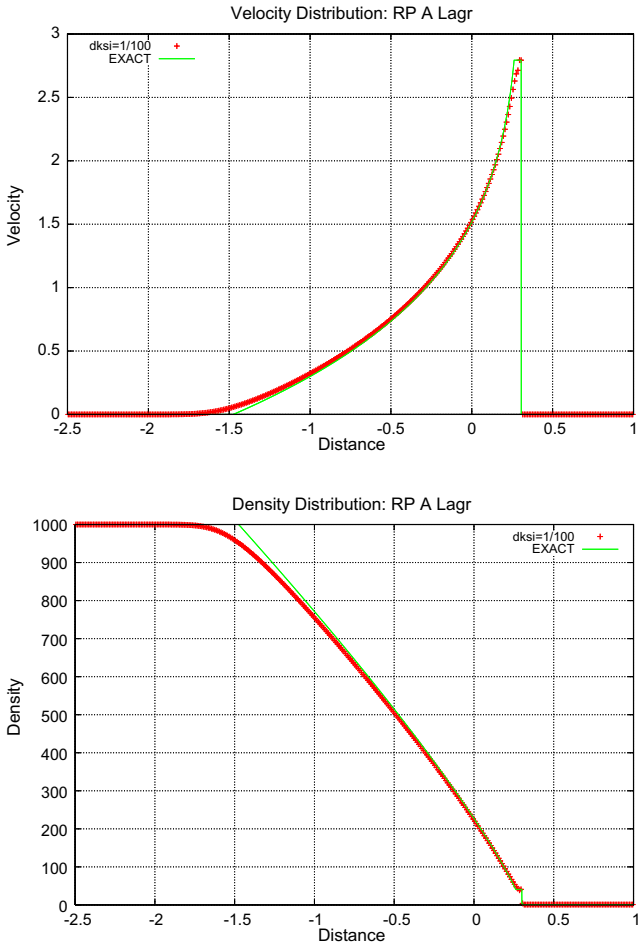

Fig. 5. Problem 1. Solution to a Riemann Problem using the present method with classical Lagrangian coordinates at $t = 0.0015$. Velocity (top) and density (bottom) distributions are presented in Lagrangian space.

The expansion waves from the examples of [1] are the *strong expansion waves with slowly moving tails.* For these types of problems the shock-capturing numerical methods do not accurately predict either pressure or density. Therefore, *even with the exactly computed entropy, the pressure and density can be incorrect.*

3.3. Contact-strength preserving

It is now clear that if and only if *all* flow variables along each side of the contact are computed correctly, will the numerical computation be correct. For general problems, this condition can hardly be achieved, but for the solution to the Riemann Problem in the unified coordinates using the shock-adaptive Godunov scheme we can *impose the constancy of the flow variables* along the left side of the contact line, i.e. in the cell containing the SRW (cell i in Fig. 1). In fact, the theoretical solution to the Riemann problem admits the constant solutions along each side of the contact line.

We emphasize that the goal of this technique is to confirm numerically the explanations given in Section 2 of the new defect of shock-capturing schemes. The contact-strength preserving technique is a cure which can be applied only to Riemann problems in the unified coordinates using the shock-adaptive Godunov scheme.

For a weak or moderate rarefaction wave, the error due to averaging over cell i (Fig. 1) is small, as explained in Section 2, so ordinary shock-capturing methods without special treatment can preserve the

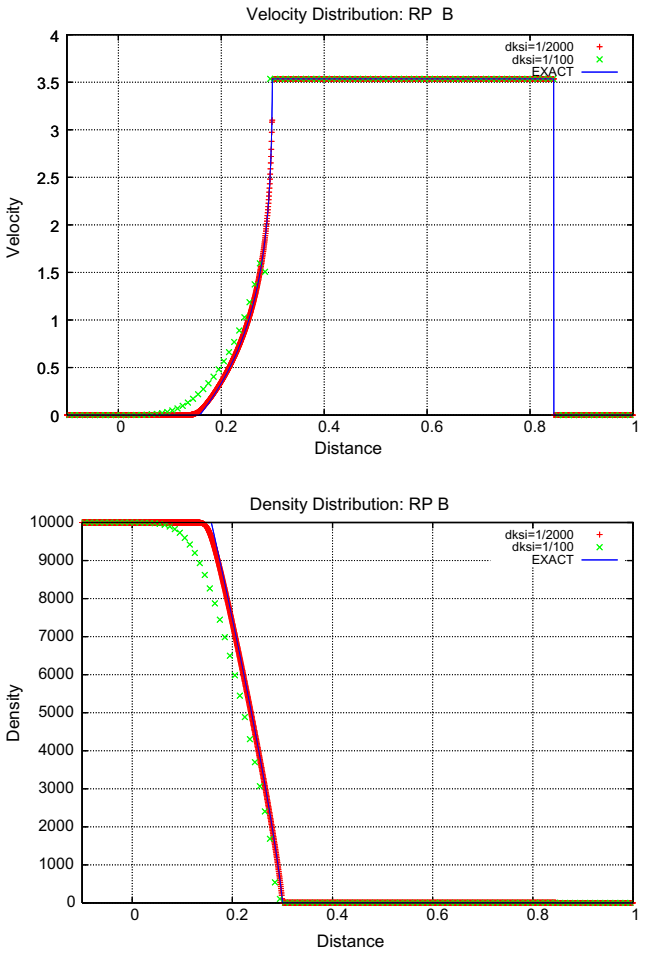

Fig. 6. Problem 2. Solution to a Riemann Problem using the present method. Velocity (top) and Density (bottom) distributions are presented in Lagrangian space.

strength of the adjacent contact with small error. This is why Problem 3 (Example 2.3 in [1]) can be computed correctly using any established method as shown in [1].

In the presence of a strong rarefaction wave, the cumulative error due to averaging over cell i is found in Section 2 to be large, violating the invariancy of flow variables on the left side (and hence also the right side through the resulting incorrect interfacial flux) of the adjacent contact.

In Fig. 2 is shown the density and entropy evolution with time in cells $(i+1)$ (next to the contact line at the right), $(i+2)$ and $(i+3)$ is shown. These results correspond to the computation of Problem 1 using the unified coordinates and the shock-adaptive Godunov scheme. We can see that the density (as well as pressure and velocity, not shown here) is incorrectly computed in all cells while the entropy is exact in the cell $(i+1)$, and it deviates from its exact value in the cells $(i+2)$ and $(i+3)$. This violation of contact strength by ordinary shock-capturing methods then produces a wrong speed, and hence wrong location for the shock wave. The cure is to preserve contact strength, and this can be done easily in our unified coordinate formulation: after the first time step, for computing the interfacial flux on the contact to be used as input to update flow in cell $(i+1)$, we simply impose the data in cell i to be the data from the exact solution to the Riemann problem in the "star" region between the tail of the expansion wave and the contact at every time step. In other words, in the subsequent Riemann problems we use, as part of the Riemann data, only the flow in the uniform flow part of the SFW-cell, instead of the whole cell, to do the averaging. This then avoids the error due to averaging over the SRW and guarantees that the strength of the contact is exactly preserved. This use of only the part of flow adjacent to the interface (contact) to do averaging is also justifiable, provided we take the time step small

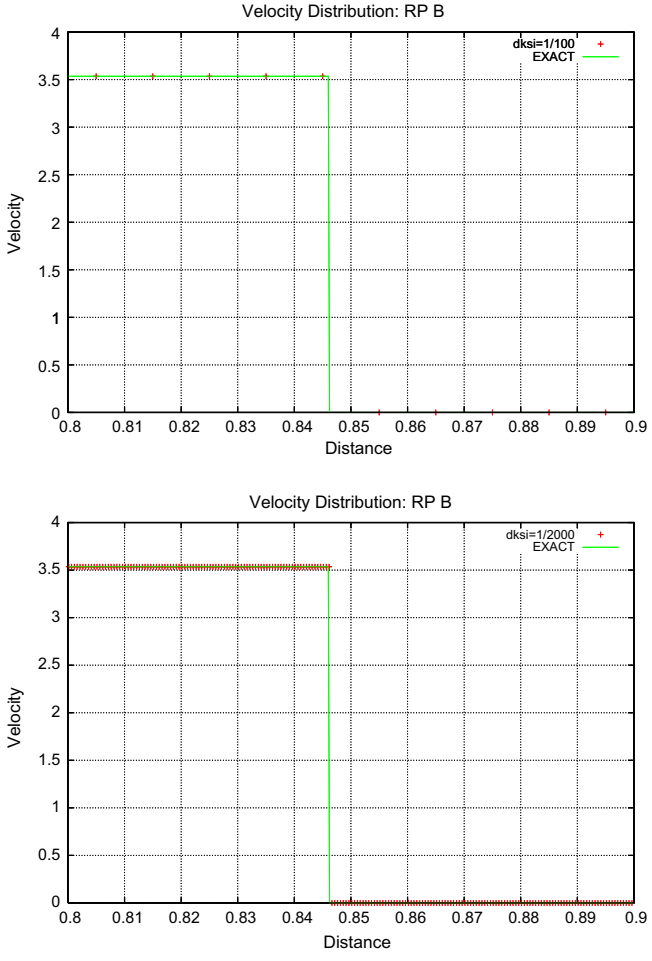

Fig. 7. Problem 2. Close-up of the velocities calculated by the present method with $d\xi = 1/100$ (top) and $d\xi = 1/1000$ (bottom).

enough so that the signal from the SRW, which is at a finite distance from the interface, has not reached the interface.

For computing the interfacial flux to be used as input to update flow in cell $(i-1)$, on the other hand, we use the average over cell i as usual.

To summarize, in our method if a shock is present, it is fitted using the information of the exact Riemann solution obtained by solving Eq. (17). The entropy jump across the shock is determined by the Riemann solution, whereas the entropy in the smooth flow region is exactly conserved by solving Eq. (21). These treat the wall overheating and other problems cited in [5] very well. If, however, the ratio of slopes, r, is very large (taken to be 10.0 in our code) in the cell next to the contact line and containing a strong rarefaction wave, we impose the flow variables from the "star" region, i.e. between the contact and the tail of the SRW.

4. Numerical results

In this section we shall present the computed results using the above described method. All computations are performed using the Godunov first-order scheme and presented in Lagrangian space together with the exact solutions for comparison.

Problem 1 (*see Section 2 for its description*). In Fig. 3 we show the velocity (top) and the density (bottom) distributions at $t = 0.15$ for the grid size, $\mathrm{d}\xi = 0.01$ and $\mathrm{d}\xi = 0.002$. The resolution of the left expansion wave is greatly improved with the refined grid, demonstrating numerical convergence. This is in the spirit of the numerical analysis: for a smooth flow, the numerical solution should approach the exact one as the grid is refined.

Fig. 4 with the close-up of the velocities computed using present method demonstrates that *the shock is resolved within a grid size*. Fig. 4 should be directly compared to Figs. 4–10 of [1] with their results for 500 cells.

Here, we shall compute the solution to Example 1 using the classical Lagrangian coordinates, i.e. for $A = \frac{\partial x}{\partial \xi} = 1/\rho$ and $h = 1$. The speed of the head of the expansion wave in these coordinates is $m_{\mathrm{Head}} = 1183$. This means that during $t = 0.15$ the head of the expansion wave will travel the distance equal to 117.5. This is an unreasonable number and we present here the solution at $t = 0.0015$. Even at this time we can see from Fig. 5 that while the head of the expansion wave made the distance 1.775, the shock wave had hardly moved, making a distance 0.006.

Problem 2 (*see Section 2 for its description*). Looking at Figs. 6 and 7 we see that the same conclusions hold as for the previous example: the resolution of the strong rarefaction wave improves with grid refinement, and the shock wave is resolved within one cell size even for rather coarse grid ($d\xi = 0.01$). Fig. 7 should be compared directly to Fig. 11 of [1] with 2000 cells.

5. Concluding remarks

In using shock-capturing methods for one-dimensional flow computation, the unified coordinates formulation, i.e., a generalized Lagrangian coordinate system with shock-adaptive Godunov scheme plus contact-strength preserving, is definitely superior to Eulerian formulation. In particular, shock and contact discontinuities are easily fitted within the over-all capturing technique with no additional cost. The new defect described in [1] can also be cured in the framework of the proposed method when applied to a Riemann problem with strong rarefaction waves.

Historically, the two seminal papers in CFD for 1D flow by Von Neumann [10] and Godunov [11] both used Lagrangian formulation. Unfortunately, this has not been easily extended to two- and three-dimensional flow, partly because it was not easy [12] to write the Lagrangian gas dynamics equations in the conservation form, and partly because the Lagrangian computation may break down due to grid tangling. Conservation form Lagrangian gas dynamics equations have now been derived [13,14], and, consequently, new Lagrangian schemes have been proposed [15], which may allow a generalization of 1D Lagrangian methods to 2- and 3D flow computation. A comprehensive review of the unified coordinates approach to CFD has just been given [16] which can also avoid grid tangling.

Appendix. Computation of m_{Head} and m_{Tail} in Eqs. (5) and (6)

The smooth solution from the $m_{\pm} = \pm\frac{a}{A}$ characteristic fields can be derived from the following system of ODE:

$$\frac{\mathrm{d}\rho}{\mathrm{d}p} = \frac{1}{a^2} \tag{22}$$

$$\frac{\mathrm{d}u}{\mathrm{d}p} = \pm\frac{1}{a\rho} \tag{23}$$

$$\frac{\mathrm{d}A}{\mathrm{d}p} = -\frac{A}{\rho a^2} \tag{24}$$

The solution for ρ, u, A relates the flow state $\mathbf{Q} = (p, \rho, u, A)^{\mathrm{T}}$ in the rarefaction fan to the initial state $\mathbf{Q}_0 = (p_0, \rho_0, u_0, A_0)^{\mathrm{T}}$ upstream of the fan through the following expressions:

$$\rho = \rho_0\left(\frac{p}{p_0}\right)^{1/\gamma} \tag{25}$$

$$u \mp \frac{2a}{\gamma - 1} = u_0 \mp \frac{2a_0}{\gamma - 1} \tag{26}$$

$$A = A_0\left(\frac{p_0}{p}\right)^{1/\gamma} \tag{27}$$

The upstream data for the left expansion wave in Problem 1 are

$$p_0 = 1000.0, \tag{28}$$

$$\rho_0 = 1000.0, \tag{29}$$

$$A_0 = 1.0, \tag{30}$$

while the pressure, p, density, ρ, and the geometrical parameter A values in the "star" region (between the tail of the left expansion wave and the contact line) are $p^* = 11.413$, $\rho^* = 40.97$, and $A^* = 24.41$, respectively. Using the above data we can deduce the values of m_{Head} and m_{Tail} as

$$m_{\text{Head}} = -\frac{a_0}{A_0} = -\frac{a_L}{A_L} = -1.1832, \tag{31}$$

$$m_{\text{Tail}} = -\frac{a^*}{A^*} = -0.0255813. \tag{32}$$

References

[1] H. Tang, Tiegang Liu, A note on the conservative schemes for the Euler equations, J. Comput. Phys. 218 (2006) 451–459.
[2] R.J. LeVeque, Nonlinear conservation laws and finite volume methods for astrophysical fluid flow, in: O. Steiner, A. Gautschy (Eds.), Computational Methods for Astrophysical Fluid Flow, Springer-Verlag, 1998.
[3] J.J. Quirk, A contribution to the great Riemann solver debate, Int. J. Num. Meth. Fluids 18 (1994) 555.
[4] W.H. Hui, S. Kudriakov, The role of coordinates in the computation of discontinuities in one-dimensional flow, Comput. Fluid Dyn. J. 8 (2000) 495–510.
[5] W.H. Hui, S. Kudriakov, On wall overheating and other computational difficulties of shock-capturing methods, Comput. Fluid Dyn. J. 10 (2001) 192.
[6] M. Shashkov, Conservative Finite-Difference Methods on General Grids, CRC Press, Boca Raton, 1996.
[7] W.H. Hui, C.Y. Loh, A new Lagrangian method for steady supersonic flow computation, Part 3: strong shocks, J. Comput. Phys. 103 (1992) 465–471.
[8] C.Y. Lapage, W.H. Hui, A shock-adaptive Godunov scheme based on the generalized Lagrangian formulation, J. Comput. Phys. 122 (1995) 291.
[9] E.F. Toro, Riemann Solvers and Numerical Methods for Fluid Dynamics, Springer, 1997.
[10] J. Von Neuman, R.D. Richtmyer, A method for the numerical calculation of hydrodynamic shocks, J. Appl. Phys. 21 (1950) 232–237.
[11] S.K. Godunov, A difference method for numerical calculation of discontinuous solutions of the equations of hydrodynamics, Mater. Sb. 47 (1959) 271–306.

[12] D. Serre, Systems of Conservation Laws, Cambridge University Press, 1999.
[13] W.H. Hui, P.Y. Li, Z.W. Li, A unified coordinate system for solving the two-dimensional Euler equations, J. Comput. Phys. 153 (1999) 596–637.
[14] W.H. Hui, S. Kudriakov, A unified coordinate system for solving the three-dimensional Euler equations, J. Comput. Phys. 172 (2001) 235.
[15] B. Despres, C. Mazeran, Lagrangian gas dynamics in two dimensions and Lagrangian systems, Arch. Ration. Mech. Anal. 178 (2005) 327.
[16] W.H. Hui, The unified coordinate system in computational fluid dynamics, Commun. Comput. Phys. 2 (2007) 577–610.